

**CONFIDENTIAL**

COPY NO.  
RM No. E8F11

21 SEP 1948

*4912*



# RESEARCH MEMORANDUM

COMPARISON OF TWO FUELS IN BUMBLEBEE 18-INCH RAM JET

INCORPORATING RAKE-TYPE FLAME HOLDER

By Fred A. Wilcox and Ephraim M. Howard

Flight Propulsion Research Laboratory  
Cleveland, Ohio

**CLASSIFICATION CANCELLED**

*and Unclassified*  
Authority *NACA Res. Abs.* Date *5/14/56*  
*RN 101*  
By *MTA 6/1/56* See \_\_\_\_\_

CLASSIFIED DOCUMENT

This document contains classified information affecting the National Defense of the United States within the meaning of the Espionage Act, USC 50:21 and 32. Its transmission or the revelation of its contents in any manner to an unauthorized person is prohibited by law. Information so classified may be imparted only to persons in the military and naval services of the United States, appropriate civilian officers and employees of the Federal Government who have a legitimate interest therein, and to United States citizens of known loyalty and discretion who of necessity must be informed thereof.

TECHNICAL  
EDITING  
WAIVED

**NATIONAL ADVISORY COMMITTEE  
FOR AERONAUTICS**

WASHINGTON  
August 18, 1948

**CONFIDENTIAL**

NACA LIBRARY  
LANGLEY MEMORIAL AERONAUTICAL  
LABORATORY  
Langley Field, Va.

## NATIONAL ADVISORY COMMITTEE FOR AERONAUTICS

RESEARCH MEMORANDUM

## COMPARISON OF TWO FUELS IN BUMBLEBEE 18-INCH RAM JET

## INCORPORATING RAKE-TYPE FLAME HOLDER

By Fred A. Wilcox and Ephraim M. Howard

## SUMMARY

An investigation to determine the performance of a Bumblebee 18-inch ram jet incorporating a rake-type flame holder was conducted using kerosene and propylene oxide as fuels. Experiments were performed in the Cleveland altitude wind tunnel at approximate pressure altitudes from 20,000 to 35,000 feet and at ram-pressure ratios equivalent to supersonic free-stream Mach numbers over the operable range of fuel-air ratios.

Use of propylene oxide improved the stability of combustion, increased the operable range of fuel-air ratios, and allowed ignition at higher values of combustion-chamber-inlet velocities. At a fuel-air ratio of about 0.070, the combustion efficiency was raised from a value of approximately 57 percent to a value of approximately 85 percent when the fuel was changed from kerosene to propylene oxide. The higher fuel-air ratios and combustion efficiencies attainable with propylene oxide, compared with those attainable with kerosene, resulted in generally higher values of gas total-temperature ratio, net thrust, and net-thrust coefficient with no appreciable change in specific fuel consumption.

## INTRODUCTION

An investigation was conducted in the NACA Cleveland altitude wind tunnel to determine the operational performance of a Bumblebee 18-inch ram jet equipped with various flame holders at high altitudes and ram-pressure ratios equivalent to supersonic free-stream Mach numbers. The flame holders, were developed as a part of the Bureau of Ordinance, Department of the Navy, Bumblebee project and were proven satisfactory during sea-level investigations (reference 1). Inasmuch as the difficulties encountered in free-flight investigations preclude a detailed study of combustion-chamber performance at high altitude, a detailed investigation was made in the Cleveland altitude wind tunnel under controlled conditions of pressure altitude and equivalent free-stream Mach number.

Altitude performance data for the best configuration employing a can-type flame holder are presented in reference 2. Performance data for the best rake-type flame holder are presented herein for a range of pressure altitudes from 20,000 to 35,000 feet and equivalent free-stream Mach numbers from 1.03 to 1.43. Most data were obtained with kerosene as fuel, but some data were obtained with propylene oxide.

Combustion-chamber performance data are presented in terms of combustion efficiency and gas total-temperature ratio across the engine as functions of the combustion-chamber-inlet variables of fuel-air ratio, velocity, and pressure. Over-all ram-jet performance is presented in terms of parameters that generalize the results to any desired operating condition in accordance with the methods presented in references 4 and 5.

#### APPARATUS AND PROCEDURE

The Bumblebee 18-inch ram jet used in the investigation was mounted above a wing that extended across the 20-foot-diameter test section of the Cleveland altitude wind tunnel (fig. 1). Air that was throttled from approximately sea-level pressure to the desired total pressure at the diffuser inlet was directly supplied to the ram jet through a pipe from the wind-tunnel make-up air system. The temperature of the inlet air was maintained at  $140^{\circ} \pm 10^{\circ} \text{ F}$  to approximate the stagnation temperatures that would be obtained at the equivalent free-stream Mach numbers investigated. A slip joint with a labyrinth air seal was attached to the diffuser inlet in order to obtain thrust measurements with the wind-tunnel balance system. Inasmuch as the engine exhausted directly into the test section, various ram-pressure ratios across the engine were obtained by varying the pressure altitude in the tunnel or by throttling the inlet air.

The ram jet consists of a subsonic diffuser containing a center body and a water-cooled combustion chamber (reference 2). The diffuser has an 11.5-inch-diameter inlet, a diffuser ratio of 1.64, and an over-all length of 9.54 feet. Attached to the diffuser was a constant-area combustion chamber having a diameter of 18 inches, a length of 5.62 feet, and a restriction to a 17.5-inch diameter at the outlet. The combustion chamber was cooled by water circulated through passages made by welding U-channels of Inconel around the outer surface.

987

The fuel-distributor system (fig. 2) was located in the rear section of the diffuser center body approximately 35 inches forward of the downstream end of the flame holder. This system consisted of two fuel patterns, designated 1 and 4 by the Applied Physics Laboratory of the Johns Hopkins University. These patterns were alternately spaced around the ram-jet center body facing in an upstream direction. The locations of the points of injection for the two fuel patterns are given in figure 2. Fuel pattern 1 gave a mixture that was rich toward the center of the diffuser annulus and spread out over a range of radii. Fuel pattern 4 discharged the fuel in a narrow band at radii slightly larger than the mean area radius of the diffuser annulus. The fuel-injector tubes had orifice diameters of approximately 0.188 inch. A drop in fuel pressure of from 12 to 20 pounds per square inch was maintained across the system for the range of fuel flows used by means of the variable-orifice-area plunger valve described in reference 3. This system provided a relatively uniform distribution of fuel to the injectors over a wide range of fuel flows with small changes in fuel-injection pressure.

A vortex-type pilot burner attached to the downstream end of the diffuser center body was used to ignite the fuel (fig. 3). Air was supplied from the diffuser through two air ducts built into the center body. This air was discharged into the pilot burner through two 45° pipe elbows, which imparted a vortex motion to the air.

The pilot combustion chamber consisted of a truncated cone 16 inches long that expanded in diameter from 6 inches at the upstream end to 7 inches at the downstream end. Fuel was supplied through a commercial spray nozzle, which was operated at approximately its rated delivery of 21.5 gallons per hour at a pressure of 100 pounds per square inch. The fuel-air mixture in the pilot was ignited by a spark plug. A tube through which hydrogen could be injected was included to aid ignition.

The flame holder, which was fitted to the downstream end of the pilot combustion chamber as shown in figure 4, consisted of six flared-tube rakes interconnected with gutters. A photograph of this flame holder after operation is shown in figure 5. Three alternate rakes were connected to a center tube, which fitted over the pilot combustion chamber, by gutters to provide a channel in which the flame could travel outward from the pilot burner to the rakes.

In order to obtain better starting characteristics and a wider range of pilot stability than afforded by kerosene, propylene oxide was used as pilot fuel. Both AN-F-32, hereinafter designated kerosene, and propylene oxide were investigated as fuels in the main burner. Some properties of each fuel are given in the following table:

Property	Kerosene AN-F-32	Propylene oxide
Heating value, Btu/lb	18,500	13,075
Approximate stoichiometric fuel-air ratio	0.068	0.105
Specific gravity	0.792-0.835	0.831
Boiling point, °F	50-percent point, 362-382	93
Flash point, °F	110	-35

Air flow through the engine was calculated from measurements of total and static pressures and indicated temperatures obtained with survey rakes mounted in the diffuser inlet. Combustion-chamber-inlet velocities were computed from air flow and wall static pressures measured at the combustion-chamber inlet. Fuel flows to the main burner and the pilot burner were determined by a rotameter and by the pressure drop across the pilot fuel nozzle, respectively. In all computations, fuel to the pilot, as well as the main burner, was included. As an alternate for the wind-tunnel balance system, jet thrust was calculated from measurements of total and static pressures obtained from a water-cooled combustion-chamber-outlet rake.

Combustion-efficiency, gas-total-temperature-rise, and engine-performance parameters were computed by the methods outlined in references 4 and 5. Heat loss to the combustion-chamber cooling water was accounted for in the calculation of combustion efficiency. This heat loss was computed from water-flow and temperature-rise measurements. The pressure loss that would occur across a normal shock at the throat of a convergent-divergent diffuser of optimum contraction ratio was added to the measured diffuser total pressure to obtain the equivalent free-stream total pressure from which the equivalent free-stream Mach numbers were computed.

Total-pressure losses across the diffuser were measured without fuel injection by means of a rake at the diffuser inlet and a rake located downstream of the fuel injector. Flame-holder total-pressure losses were determined from total pressures measured with the rake behind the fuel injector and the combustion-chamber-outlet rake.

987

Data were obtained with kerosene at an approximate pressure altitude of 30,000 feet over the operable range of combustion-chamber-inlet static pressures and fuel-air ratios. In addition, two data points were obtained with kerosene at a pressure altitude of approximately 35,000 feet and with reduced combustion-chamber-inlet static pressure. With propylene oxide, two data points were obtained at an altitude of approximately 20,000 feet and one point at approximately 30,000 feet. When possible, lean and rich blow-out points were determined for each fuel.

## SYMBOLS

The following symbols are used in this report:

- A cross-sectional area, square feet
- $C_F$  net-thrust coefficient,  $\frac{F_n}{q_0 A_3}$
- $F_j$  jet thrust, pounds
- $F_n$  net thrust, pounds
- $f/a$  fuel-air ratio
- M Mach number
- P total pressure, pounds per square foot absolute
- $\Delta P$  total pressure drop, pounds per square foot
- p static pressure, pounds per square foot absolute
- q dynamic pressure, pounds per square foot
- T total temperature, °R
- V velocity, feet per second
- $W_a$  air flow, pounds per second
- $W_f$  fuel flow, pounds per hour
- $\delta$  ratio of absolute tunnel ambient-air pressure to absolute static pressure at NACA standard atmospheric conditions at sea level,  $p_0/2116$

- $\eta$  over-all efficiency, percent
- $\eta_b$  combustion efficiency, percent
- $\theta$  ratio of absolute total temperature at diffuser inlet to absolute static temperature at NACA standard atmospheric conditions at sea level,  $T_1/519$
- $\tau$  ratio of absolute total temperature at combustion-chamber outlet to absolute total temperature at diffuser inlet,  $T_4/T_1$

Subscripts:

- 0 equivalent free-stream conditions
- 1 subsonic diffuser inlet
- 2 diffuser outlet and combustion-chamber inlet
- 4 combustion-chamber outlet
- j exhaust jet at ambient pressure ( $p_j = p_0$ )

RESULTS AND DISCUSSION

Ram-jet performance data obtained over the operable range of fuel-air ratios and with two fuels for combustion-chamber-outlet conditions at or near choking are presented. The ranges of fuel-air ratio  $f/a$  and combustion-chamber-inlet static pressure  $p_2$  and velocity  $V_2$  over which the engine was operated are shown in table I.

The blow-out data shown in table I represent the minimum and maximum  $f/a$  at which combustion could be maintained in the engine. The ranges of inlet conditions over which the blow-out data were obtained are shown by the values of  $p_2$  and  $V_2$  in table I. With kerosene as the fuel, the operable range of  $f/a$  narrowed as  $p_2$  was reduced from 1922 to 1000 pounds per square foot absolute. At this lower  $p_2$ , lean and rich blow-out points were almost coincident.

For the range of combustion-chamber-inlet conditions investigated, the operable range of fuel-air ratios with propylene oxide as a fuel and the range of percentage stoichiometric fuel-air ratio were wider than with kerosene. No additional data were obtained

with propylene oxide because of the limited quantity of fuel available. At maximum  $p_2$ , the rich blow-out limit could not be obtained with propylene oxide because the fuel pump used could not deliver the fuel rates required.

Operation was satisfactory over the entire operable range of fuel-air ratios for each fuel. Use of propylene oxide improved stability of combustion, increased the operable range of  $f/a$ , and permitted ignition at higher  $V_2$ .

#### Ram-Jet Combustion Performance

The relations between combustion-chamber parameters, combustion efficiency  $\eta_b$ ,  $V_2$ ,  $p_2$ , gas total-temperature ratio  $\tau$ , and  $f/a$ , are presented in figures 6 to 8. In figure 6,  $\eta_b$  and  $\tau$  are presented as functions of  $f/a$ . Values of  $V_2$  at which the data were taken are indicated for the  $\eta_b$  data points. Combustion efficiencies obtained with propylene oxide were higher than those obtained with kerosene. At an  $f/a$  of about 0.070 and  $V_2$  of approximately 240 feet per second,  $\eta_b$  was raised from an approximate value of 57 percent to a value of about 85 percent when the fuel was changed from kerosene to propylene oxide. Over the range of  $f/a$  investigated for both fuels,  $\eta_b$  decreased as  $f/a$  increased. At a constant value of  $f/a$ , the value of  $\tau$  obtained with both fuels was approximately the same. Higher values of  $\tau$  were obtained with propylene oxide than with kerosene because burning with high combustion efficiencies was maintained at higher  $f/a$ .

With kerosene at approximately constant values of  $V_2$  and  $f/a$ , variations in  $p_2$  appeared to have little effect on  $\eta_b$  over the range of  $p_2$  for which data at constant  $V_2$  and  $f/a$  were obtained (fig. 7). This effect is similar to results reported in previous investigations (references 2 and 6).

Inasmuch as  $p_2$  had negligible effect on  $\eta_b$  over the range investigated, the data in figure 8, which show the effects of  $V_2$ , were selected only for constant  $f/a$ . At an  $f/a$  of 0.068,  $\eta_b$  decreased from a value of about 63 percent to a value of 54 percent as  $V_2$  was raised from 230 to 247 feet per second. This decrease in  $\eta_b$  was presumably due to the reduced time available for combustion with increased  $V_2$ . At a  $V_2$  of approximately 246 feet per



second,  $\eta_b$  was reduced from a value of about 64 percent to a value of about 54 percent when the  $f/a$  was increased from 0.058 to 0.068. The main cause of this decrease in  $\eta_b$  was believed to be local overenrichment of the fuel-air mixture.

#### Ram-Jet Over-All Performance

Ram-jet over-all performance parameters are presented as functions of equivalent free-stream Mach number  $M_0$  in figures 9 to 16. Jet thrust  $F_j$  and jet thrust reduced to NACA standard atmospheric conditions at sea level,  $F_j/\delta$  are shown in figure 9. Approximate pressure altitudes at which the data were taken are shown in figure 9(a). At constant  $M_0$ ,  $F_j$  increased as the pressure altitude was reduced. Both  $F_j$  and  $F_j/\delta$  increased as  $M_0$  was raised. A single curve has been faired through the  $F_j/\delta$  data for both rake and scale measurements.

Reduced net thrust  $F_n/\delta$  and net-thrust coefficient  $C_F$  are shown in figure 10. Both  $F_n/\delta$  and  $C_F$  increased with increasing  $M_0$  and also with increasing  $\tau$ . The highest value of  $F_n/\delta$  reached in the investigation (3890 lb) was attained at an  $M_0$  of 1.42 and a  $\tau$  of 5.1 with propylene oxide as the fuel. At this condition, the value of  $C_F$  was 0.733. At an  $M_0$  approximately equal to 1.1,  $C_F$  was increased from an approximate value of 0.47 to 0.64 by increasing the value of  $\tau$  from 4.4 to 6.0. Inasmuch as the use of propylene oxide permitted the attainment of higher values of  $\tau$ , higher values of  $F_n/\delta$  and  $C_F$  could have been obtained at high  $M_0$  if more propylene oxide had been available.

The trends in reduced air specific impulse with variations in  $M_0$  or  $\tau$  (fig. 11) are similar to those in  $F_n/\delta$  and  $C_F$  (fig. 10). At a constant value of  $\tau$ , the reduced air specific impulse increased as  $M_0$  was raised. The maximum value of reduced air specific impulse obtained was 48 pounds net thrust per pound air per second; this value was obtained at the same conditions as the maximum  $F_n/\delta$  and  $C_F$ . At an  $M_0$  of approximately 1.1, the reduced air specific impulse was increased from about 26.5 to about 42.5 pounds net thrust per pound air flow per second by raising the value of  $\tau$  from 4.4 to 6.0.

Data for the specific fuel consumption reduced to sea-level conditions are shown in figure 12. Inasmuch as several curves of constant  $\eta_b$  and  $\tau$  would be required for each fuel to correlate the data, these curves are omitted for clarity and the values of  $\eta_b$  and  $\tau$  are noted beside the points. As  $M_0$  increased, the specific fuel consumption reduced to sea-level conditions decreased. Because of the higher heating value of the kerosene, no appreciable difference was obtained between the values of the reduced specific fuel consumptions for the two fuels. On a volumetric basis, the reduced specific fuel consumptions would be nearly equal for the two fuels because of their nearly equal densities.

Over-all efficiency and ideal over-all efficiency are shown in figure 13. As in the case of specific fuel consumption reduced to sea-level conditions, over-all-efficiency curves at constant  $\eta_b$  and  $\tau$  for each fuel are not presented. These data were generalized to one curve of ideal over-all efficiency (fig. 13(b)) by methods outlined in reference 5. As  $M_0$  was raised, the over-all efficiency increased over the range investigated. The highest over-all efficiency (10.4 percent) was obtained at the same conditions as the maximum  $F_n/\delta$ ,  $C_F$ , and reduced air specific impulse. At an  $M_0$  of about 1.43, the over-all efficiency was raised from a value of about 8.0 percent to a value of about 10.4 percent when the fuel was changed from kerosene to propylene oxide. This increase primarily resulted from the improved combustion efficiency.

Exhaust-jet Mach number  $M_0$  and combustion-chamber-inlet Mach number parameter  $M_2\sqrt{\tau}$  are presented in figures 14 and 15, respectively. Combustion-chamber-outlet choking  $M_j \geq 1$  occurred at  $M_0$  equal to or greater than approximately 1.20. Over the range investigated,  $M_j$  increased in an almost linear manner with  $M_0$ . The value of  $M_2\sqrt{\tau}$  had an essentially constant value of approximately 0.445 over the range of  $M_0$  investigated.

The total-pressure ratio across the engine  $P_j/P_0$  is presented in figure 16. The essentially constant relation between  $P_j/P_0$  and  $M_0$  was obtained because the ram jet was operated at or near combustion-chamber-outlet choking conditions. Included in  $P_j/P_0$  is the assumed supersonic-diffuser-recovery ratio, which is 0.99 at an  $M_0$  of 1.40. Discussions and evaluations of the various types of pressure loss in ram jets are given in references 5 and 7.

Measured total-pressure-drop coefficients, expressed as the ratio of total-pressure drop to impact pressure at the combustion-chamber

inlet, were obtained from drag studies without combustion across the subsonic diffuser with the fuel injector in place and across the flame holder and the combustion chamber. These coefficients are presented in figure 17 as functions of the combustion-chamber-inlet Mach number  $M_2$ . The total-pressure-drop coefficient for the subsonic diffuser increased with  $M_2$  from a value of about 1.5 at  $M_2$  of about 0.07 to a value of approximately 2.2 at an  $M_2$  of about 0.30. Over the same range of  $M_2$ , the total-pressure-drop coefficient across the flame holder and the combustion chamber was approximately constant at about 1.45.

#### SUMMARY OF RESULTS

The following results were obtained from an investigation of a Bumblebee 18-inch ram jet equipped with a rake-type flame holder and operating at pressure altitudes from approximately 20,000 to 35,000 feet and at ram-pressure ratios equivalent to supersonic free-stream Mach numbers with kerosene and propylene oxide as fuels:

1. An improvement in combustion efficiency was noted when propylene oxide was substituted for kerosene as the fuel. At a fuel-air ratio of approximately 0.070, the combustion efficiency was raised from a value of approximately 57 percent to a value of about 85 percent when the fuel was changed from kerosene to propylene oxide. At this fuel-air ratio, approximately equal values of gas total-temperature ratios across the engine were obtained.

2. The use of propylene oxide in place of kerosene improved the stability of combustion, permitted ignition at higher values of combustion-chamber-inlet velocities, and increased the range of fuel-air ratios at which combustion could be maintained. Higher values of fuel-air ratio and combustion efficiency attainable with propylene oxide resulted in generally higher values of gas total-temperature ratio, net thrust, and net-thrust coefficient.

3. Values of specific fuel consumption reduced to sea-level conditions obtained with kerosene, and with propylene oxide were inappreciably different because of the higher heating value of kerosene.

Flight Propulsion Research Laboratory,  
National Advisory Committee for Aeronautics  
Cleveland, Ohio.

## REFERENCES

1. Anon.: Survey of the Bumblebee. Bumblebee Rep. No. 31, Appl. Physics Lab., Johns Hopkins Univ., Feb., 1946. (U.S. Navy Contract NOrd 7386.)
2. Sterbentz, W. H., and Nussdorfer, T. J.: Investigation of Performance of an 18-Inch Bumblebee Ram Jet with a Can-Type Flame Holder. NACA RM No. E8E21, 1948.
3. Anon.: Bumblebee Equipment Manual. Bumblebee Series Rep. No. 62, Appl. Physics Lab., Johns Hopkins Univ., Nov. 1947. (U.S. Navy Contract NOrd 7386.)
4. Perchonok, Eugene, Wilcox, Fred A., and Sterbentz, William H.: Preliminary Development and Performance Investigation of a 20-Inch Steady-Flow Ram Jet. NACA RM No. E6D05, 1946.
5. Perchonok, Eugene, Sterbentz, William H., and Wilcox, Fred A.: Performance of a 20-Inch Steady-Flow Ram Jet at High Altitudes and Ram-Pressure Ratios. NACA RM No. E6L06, 1947.
6. Sterbentz, W. H., Perchonok, E., and Wilcox, F. A.: Investigation of Effects of Several Fuel-Injection Locations on Operational Performance of a 20-Inch Ram Jet. NACA RM No. E7L02, 1948.
7. Williams, Glenn C., and Quinn, John C.: Ram Jet Power Plants. Jet Propelled Missiles Panel, OSRD, May 1945. (Under Assignment to Coordinator of Research and Development, U.S. Navy.)

TABLE I - RANGE OF OPERATION FOR INVESTIGATION OF RAKE-TYPE FLAME HOLDER

IN BUMBLEBEE 18-INCH RAM JET

Fuel	Combustion-chamber-inlet static pressure, $P_2$ (lb/sq ft abs.)	Lean limit			Rich limit		
		Fuel-air ratio $f/a$	Percentage stoichiometric	Combustion-chamber-inlet velocity, $V_2$ (ft/sec)	Fuel-air ratio $f/a$	Percentage stoichiometric	Combustion-chamber-inlet velocity, $V_2$ (ft/sec)
Kerosene (AN-F-32)	1785 - 1922	0.047	69	279	0.072	106	230
	1396 - 1427	.047	69	263	.072	106	250
	1193 - 1209	.057	84	269	.067	99	247
	1000	.062	91	---	.062	91	---
Propylene oxide	1803 - 1955	0.050	48	285	(a)	(a)	---
	1350 - 1400	.030	29	336	0.107	102	174

<sup>a</sup>Rich limit not determined.

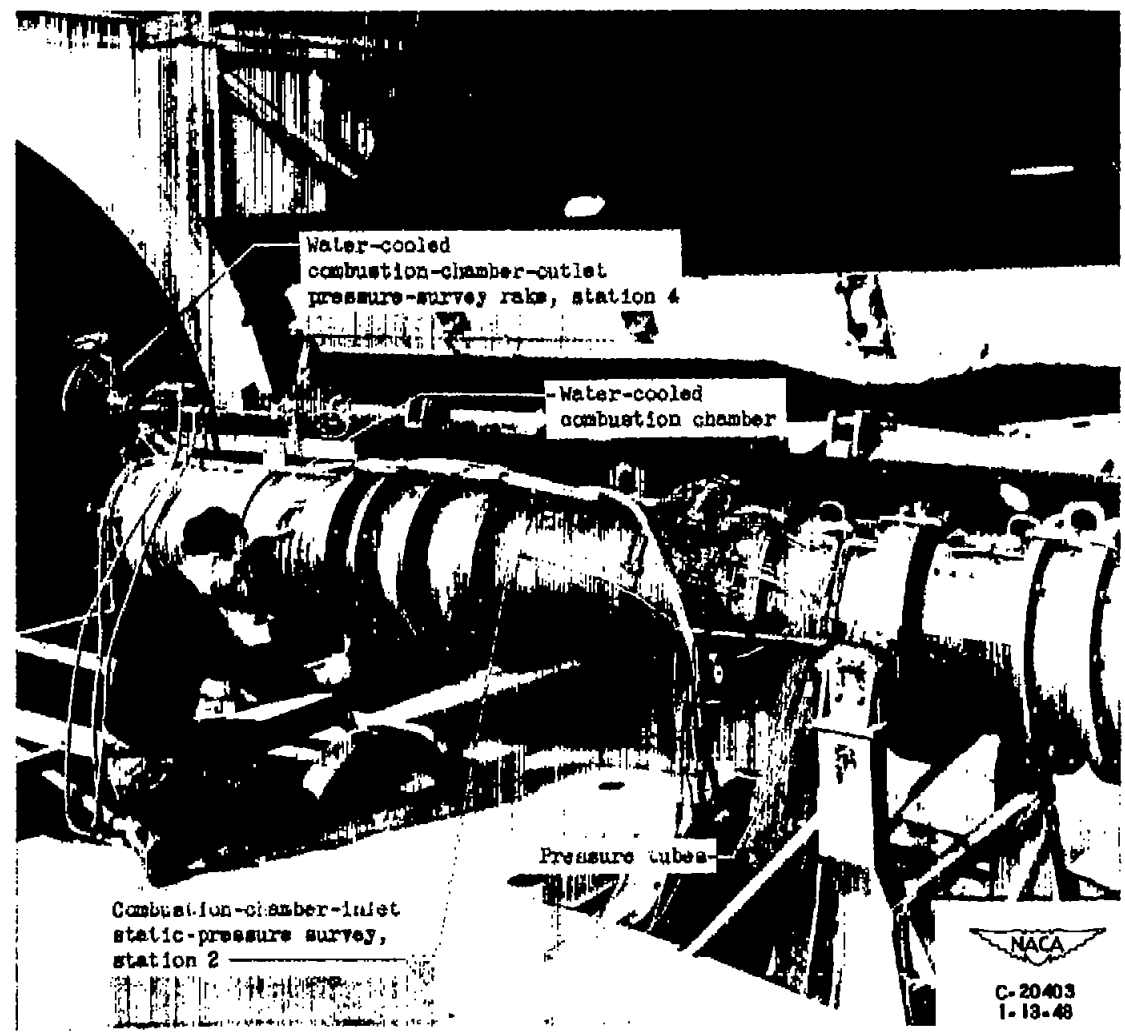


Figure 1. - Installation of Bumblebee 18-inch ram jet in altitude wind tunnel.

.

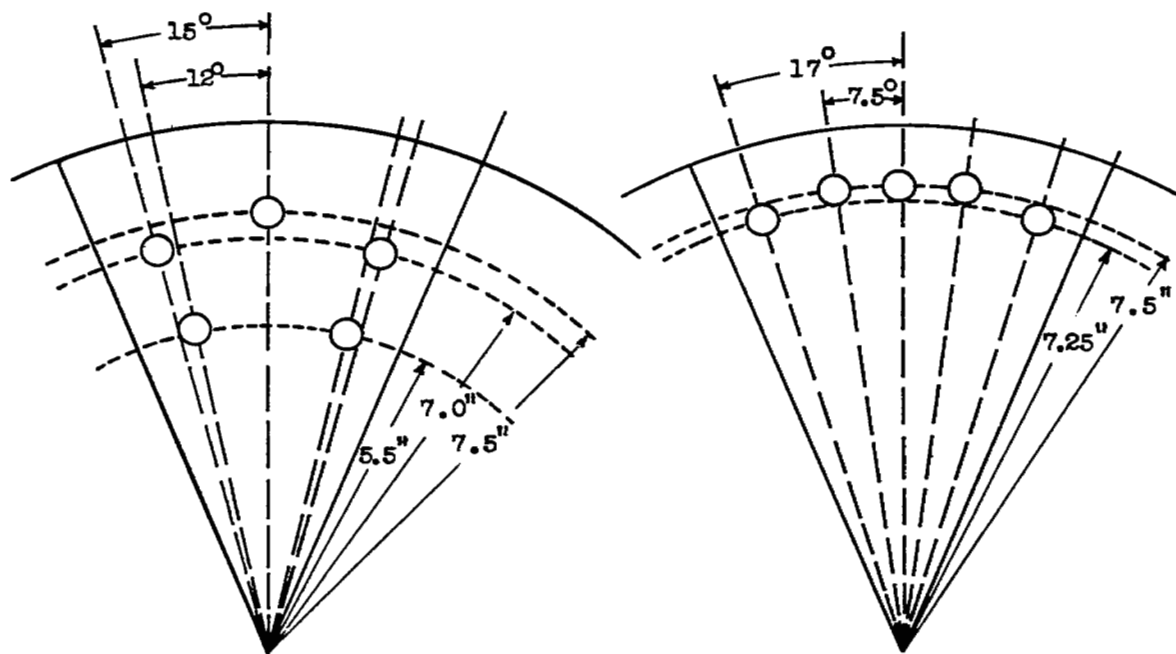
.

.

.

.

.



Fuel pattern 1

Fuel pattern 4

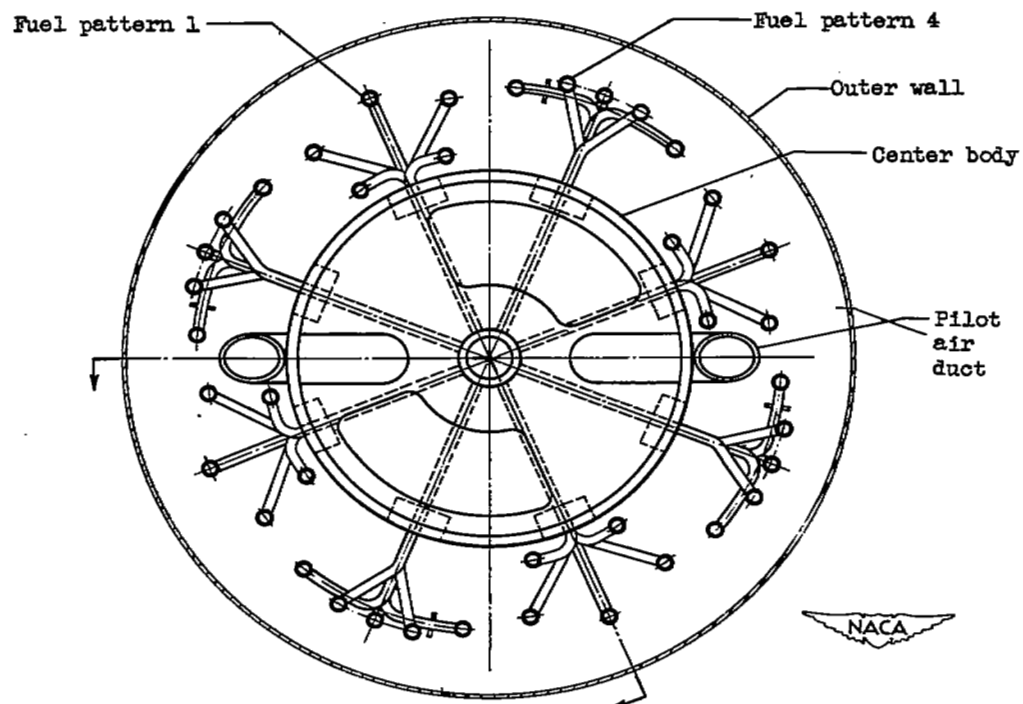
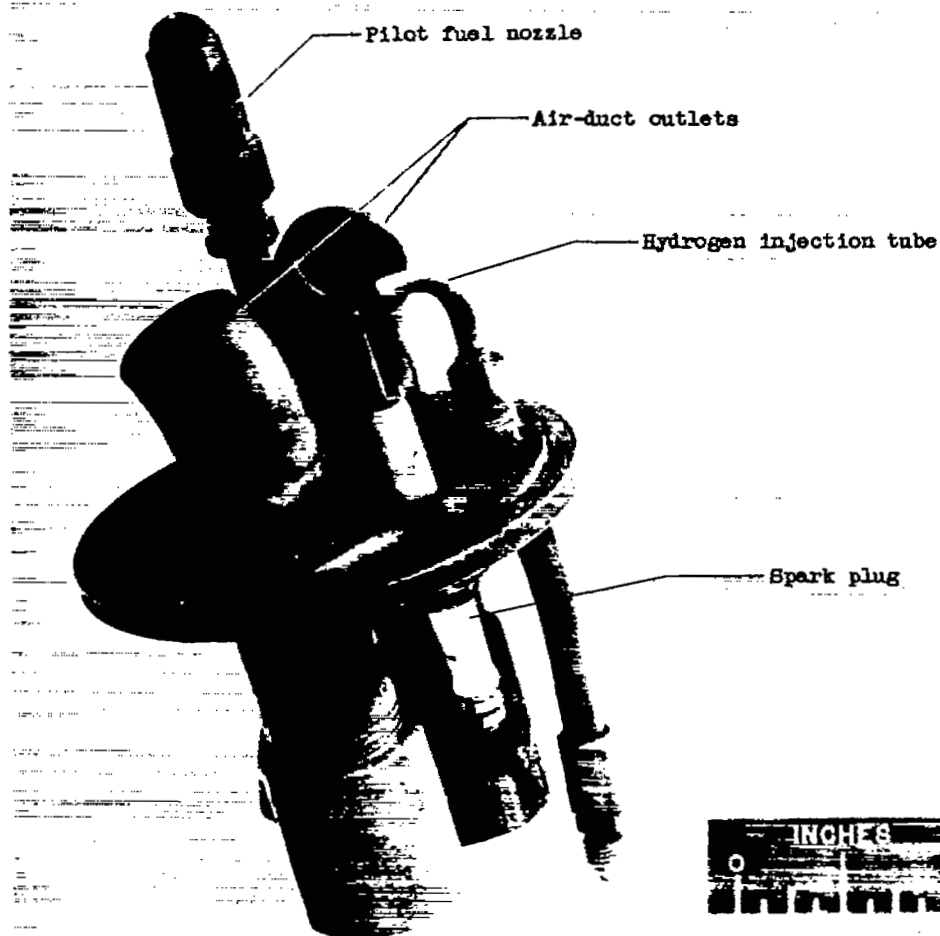


Figure 2. - Schematic diagram of fuel-distributor system showing locations of injector tubes.







NACA  
C-20400  
1-12-48

Figure 3. - Vortex pilot burner for Bumblebee 18-inch ram jet.



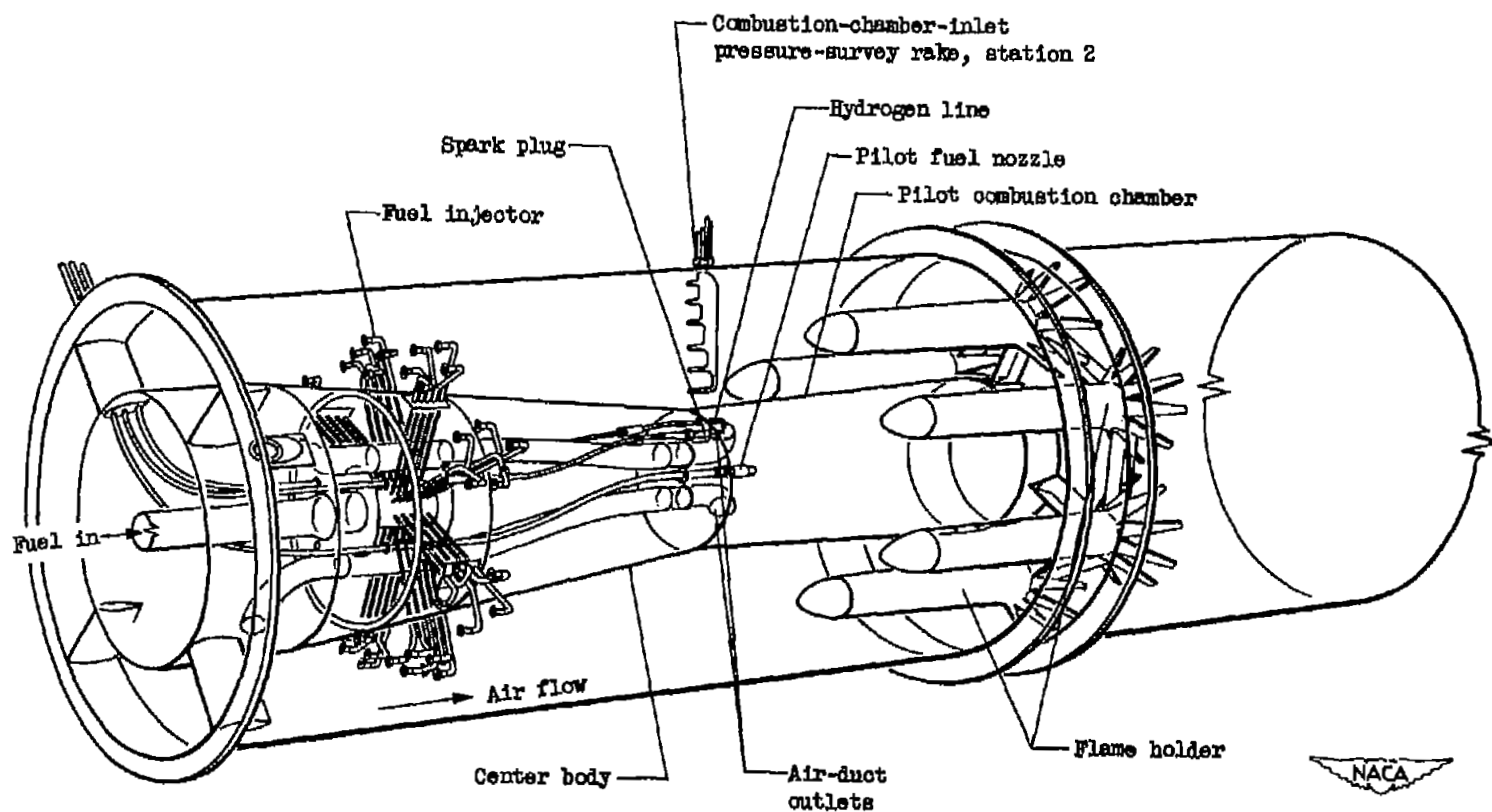


Figure 4. - Schematic diagram of installation of rake-type flame holder in Bumblebee 18-inch ram jet.





Figure 5. - Rake-type flame holder after operation in Bumblebee 18-inch ram jet.



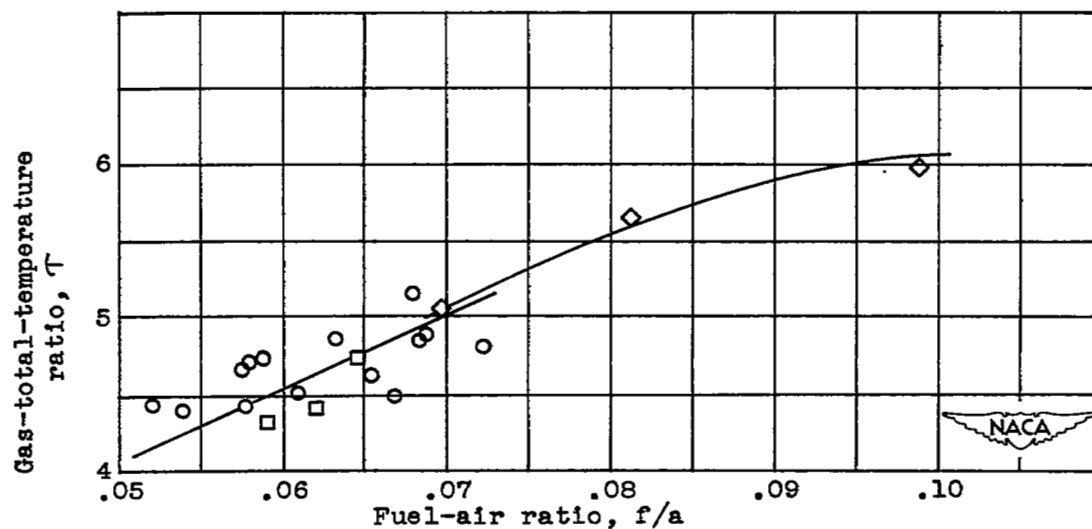
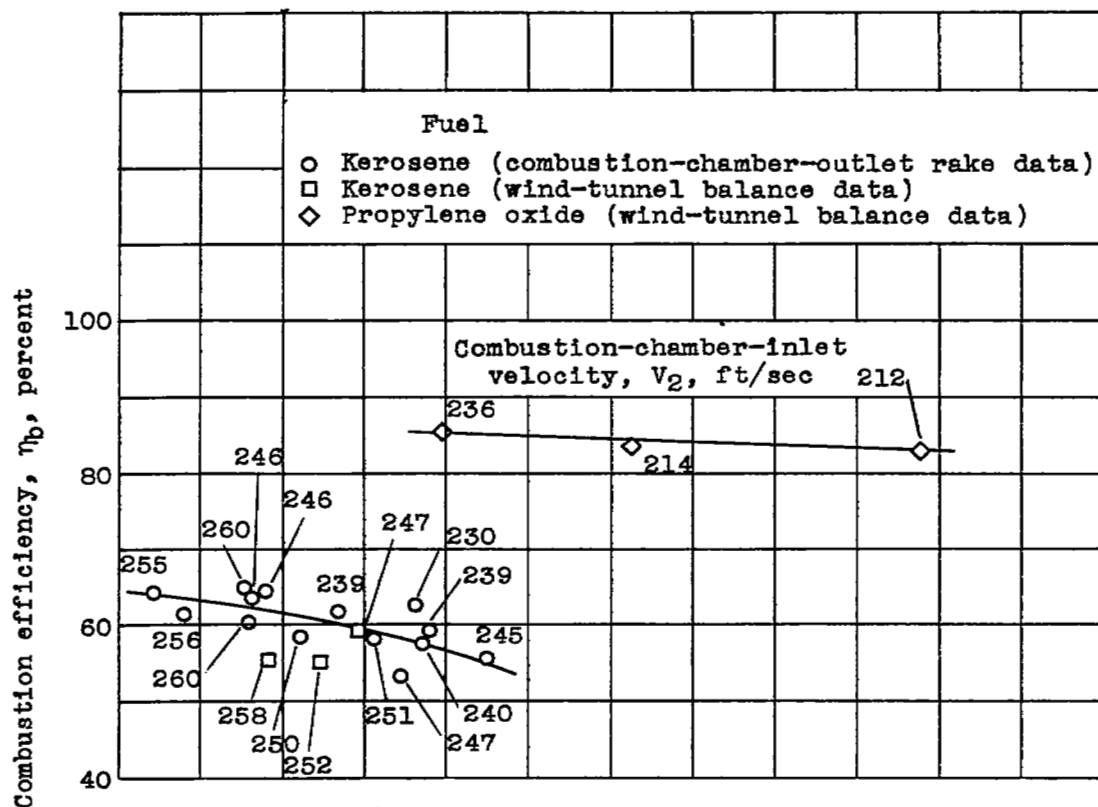


Figure 6. - Effect of fuel-air ratio on combustion efficiency and gas total-temperature ratio. Combustion-chamber-inlet static pressure, 1193 to 1955 pounds per square foot absolute; combustion-chamber-inlet velocity, 212 to 260 feet per second.



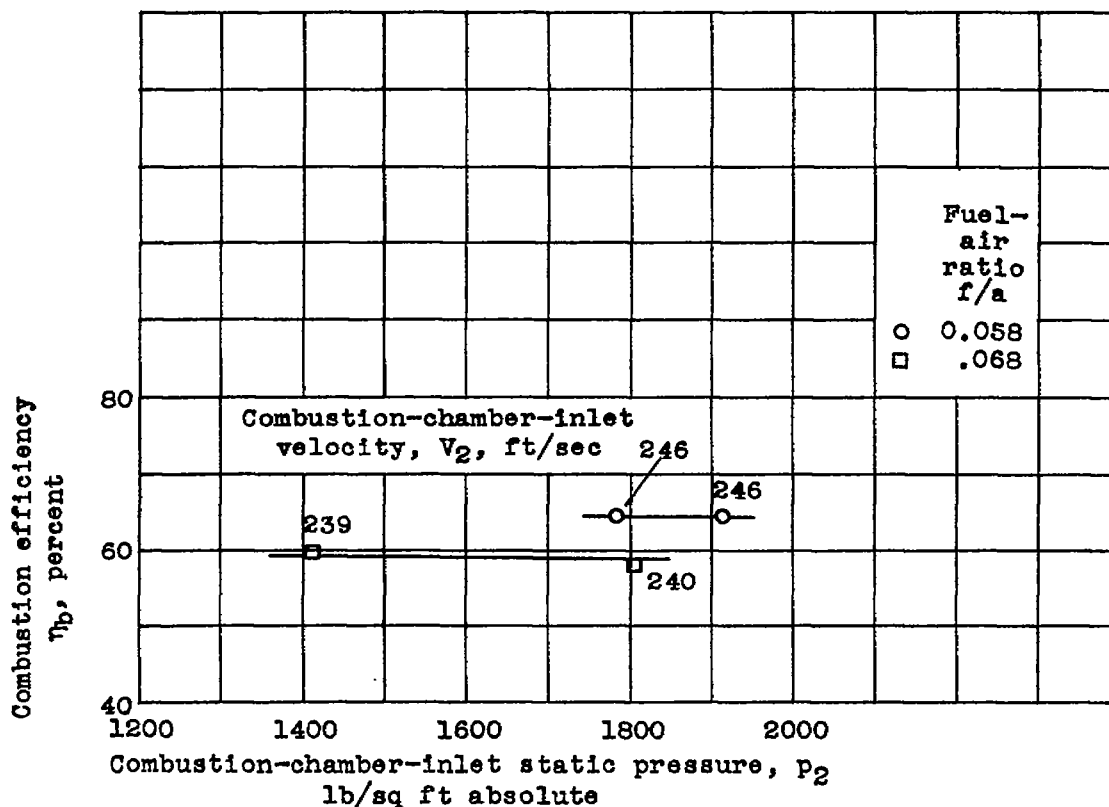


Figure 7. - Effect of combustion-chamber-inlet static pressure on combustion efficiency. Fuel, kerosene.

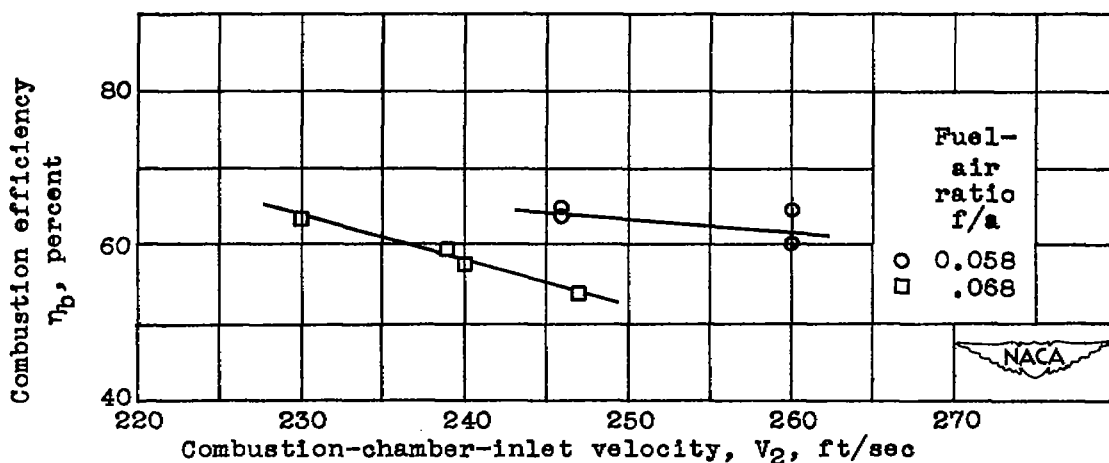
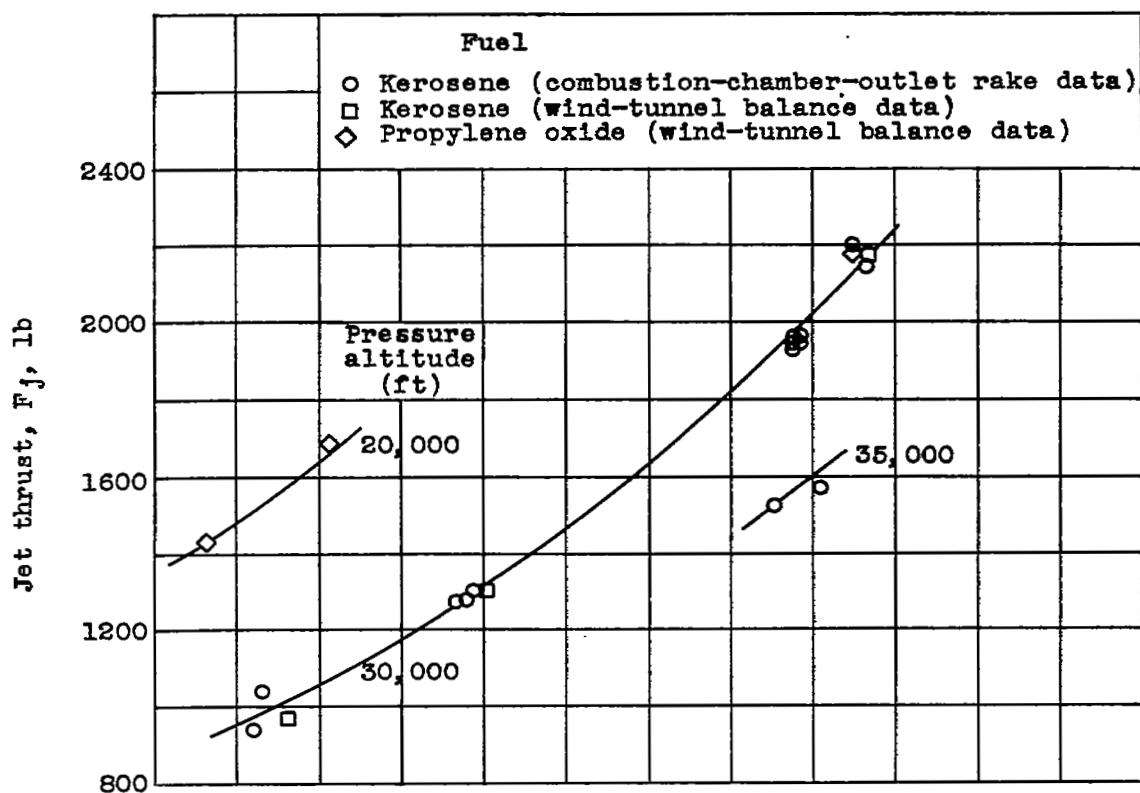
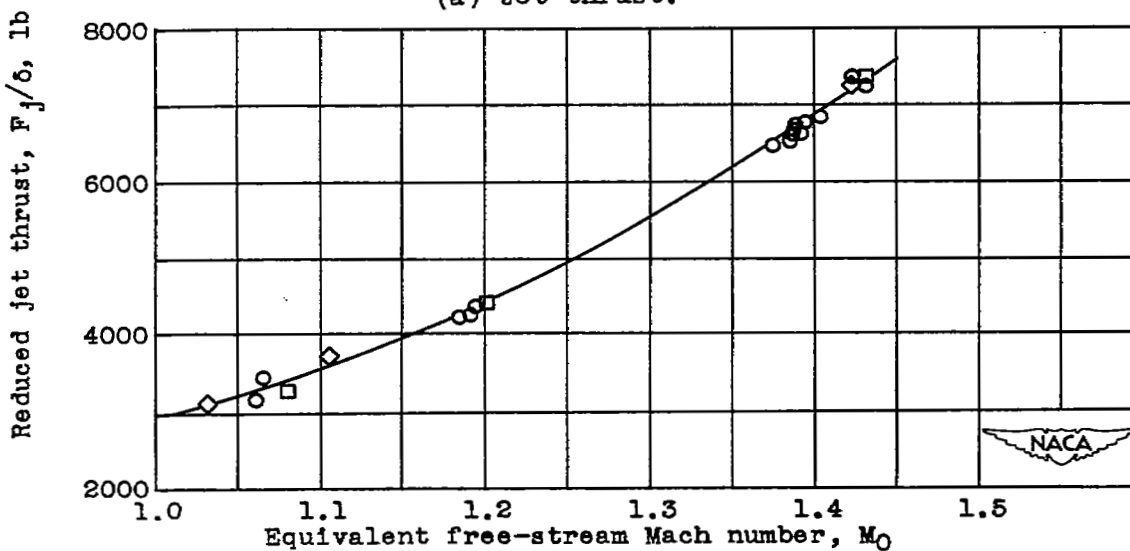


Figure 8. - Effect of combustion-chamber-inlet velocity on combustion efficiency. Combustion-chamber-inlet static pressure, 1195 to 1913 pounds per square foot absolute; fuel, kerosene.

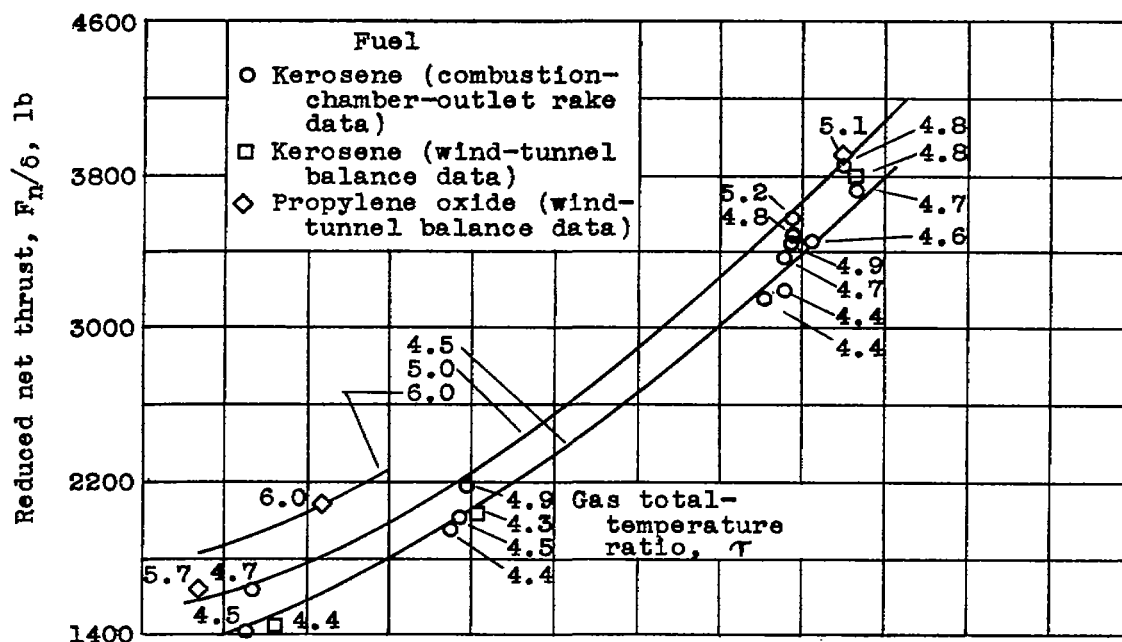


(a) Jet thrust.

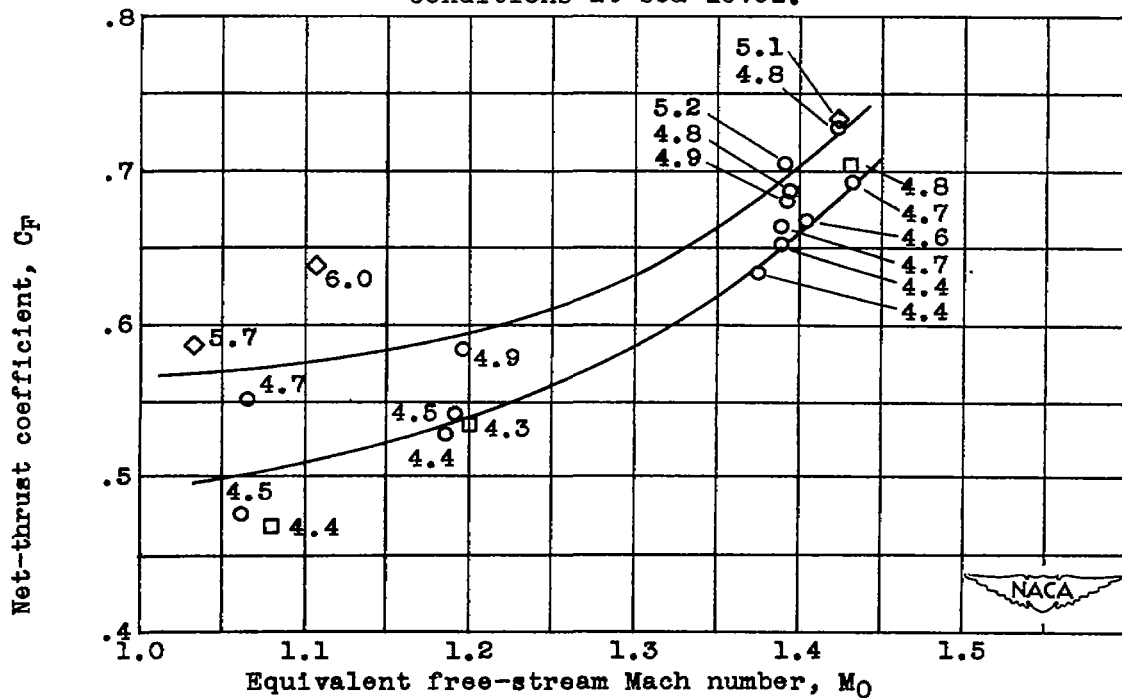


(b) Jet thrust reduced to NACA standard atmospheric conditions at sea level.

Figure 9. - Effect of equivalent free-stream Mach number on jet thrust and reduced jet thrust.



(a) Net thrust reduced to NACA standard atmospheric conditions at sea level.



(b) Net-thrust coefficient.

Figure 10. - Effects of equivalent free-stream Mach number and gas total-temperature ratio on reduced net thrust and net-thrust coefficient.

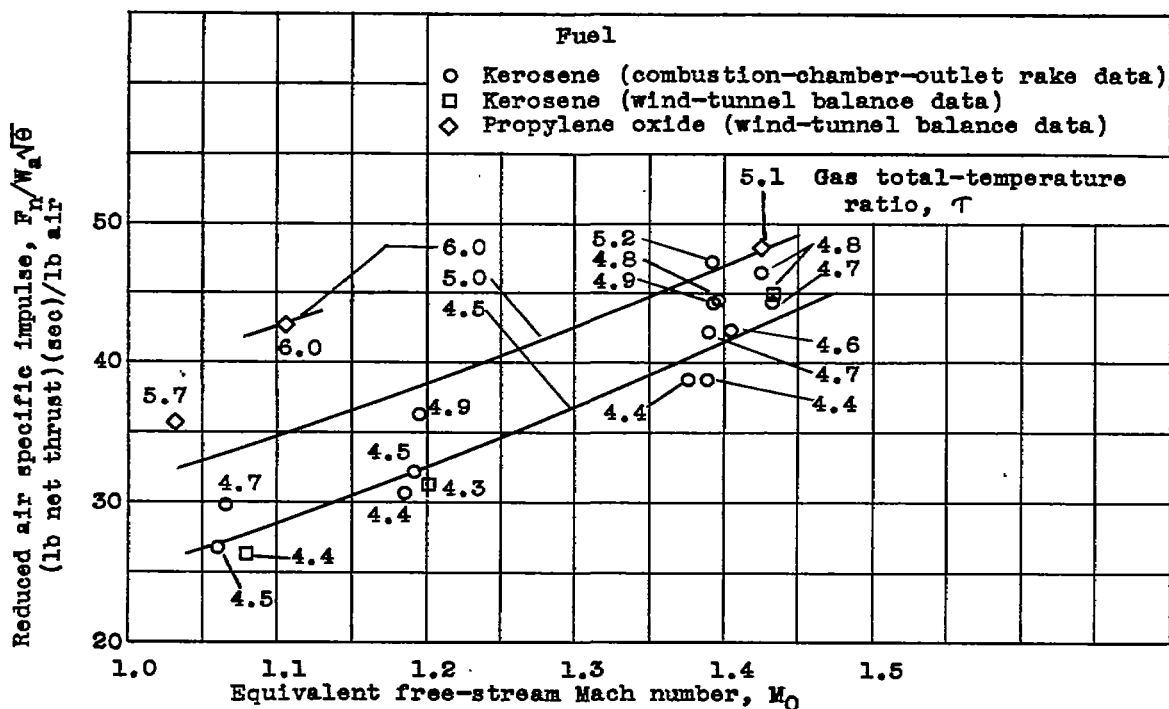


Figure 11. - Effects of equivalent free-stream Mach number and gas total-temperature ratio on air specific impulse reduced to NACA standard atmospheric conditions at sea level.

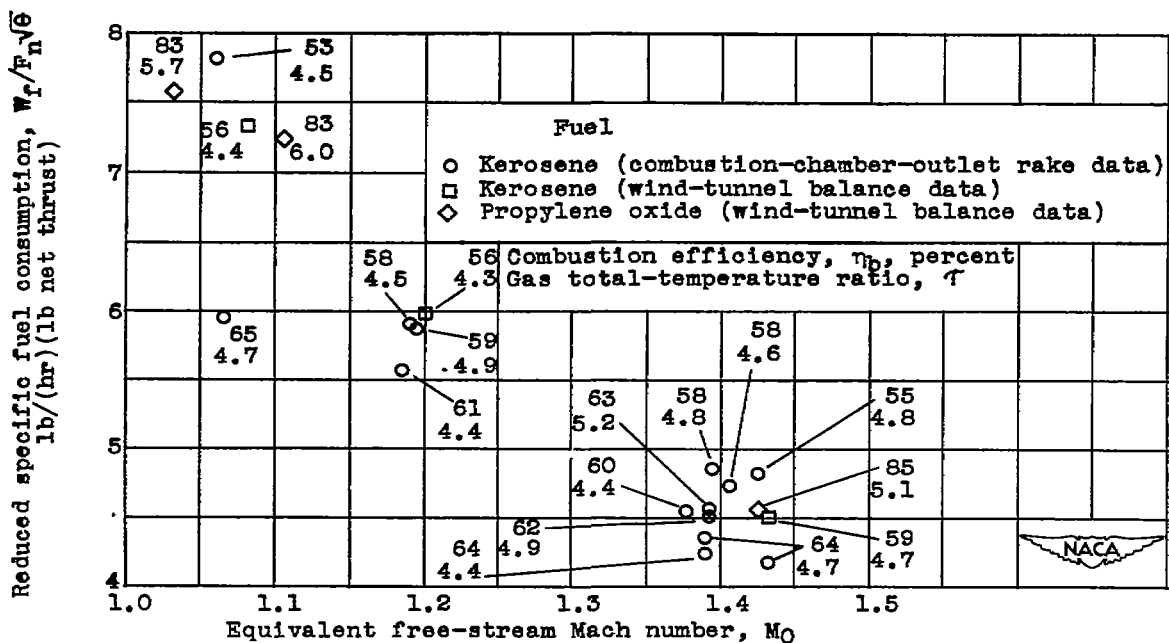


Figure 12. - Effect of equivalent free-stream Mach number on specific fuel consumption reduced to NACA standard atmospheric conditions at sea level.



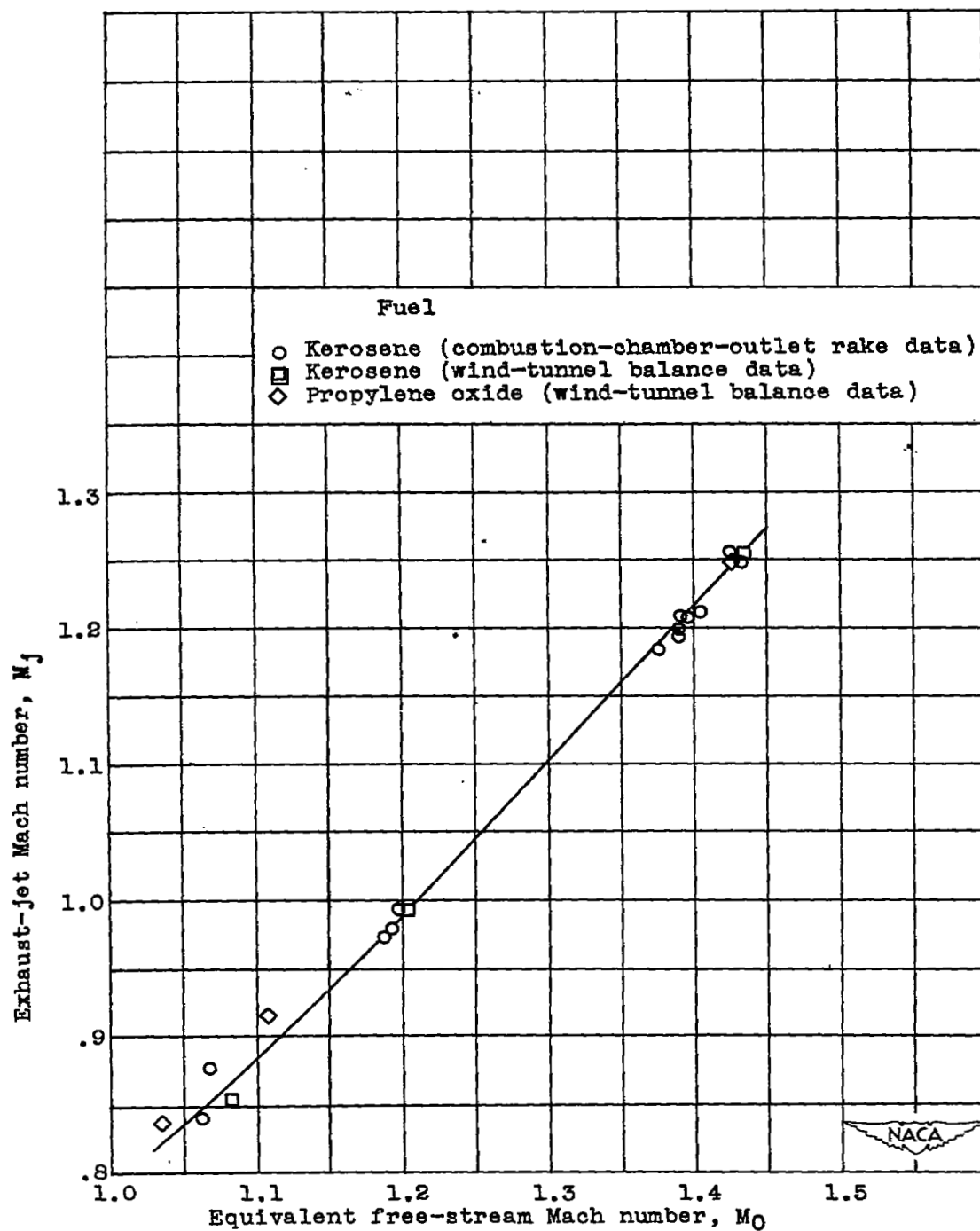


Figure 14. - Effect of equivalent free-stream Mach number on exhaust-jet Mach number.

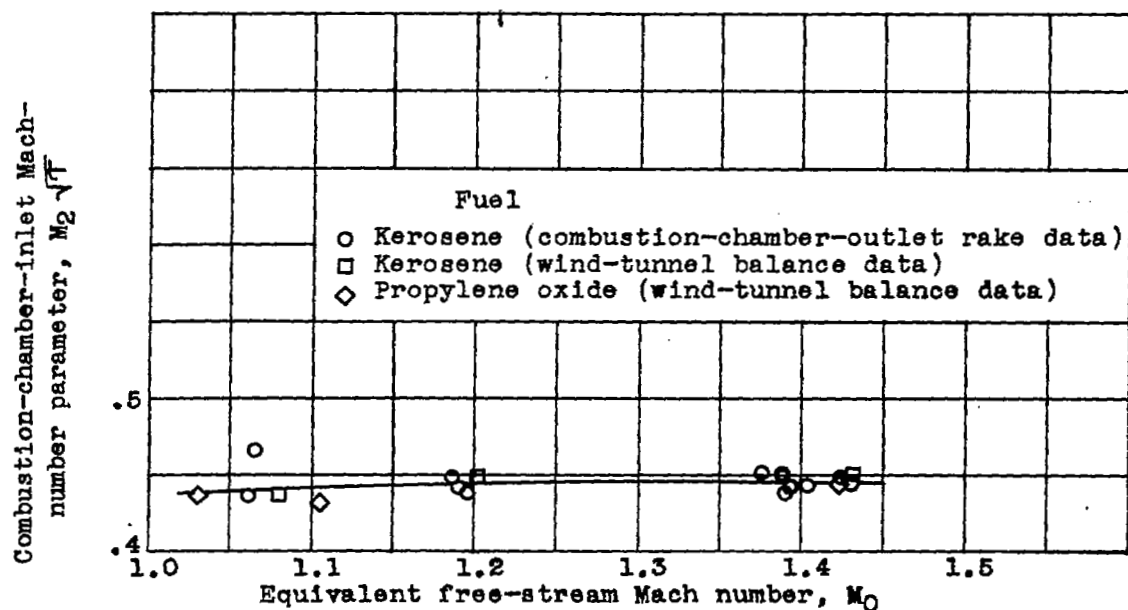


Figure 15. - Effect of equivalent free-stream Mach number on combustion-chamber-inlet Mach-number parameter.

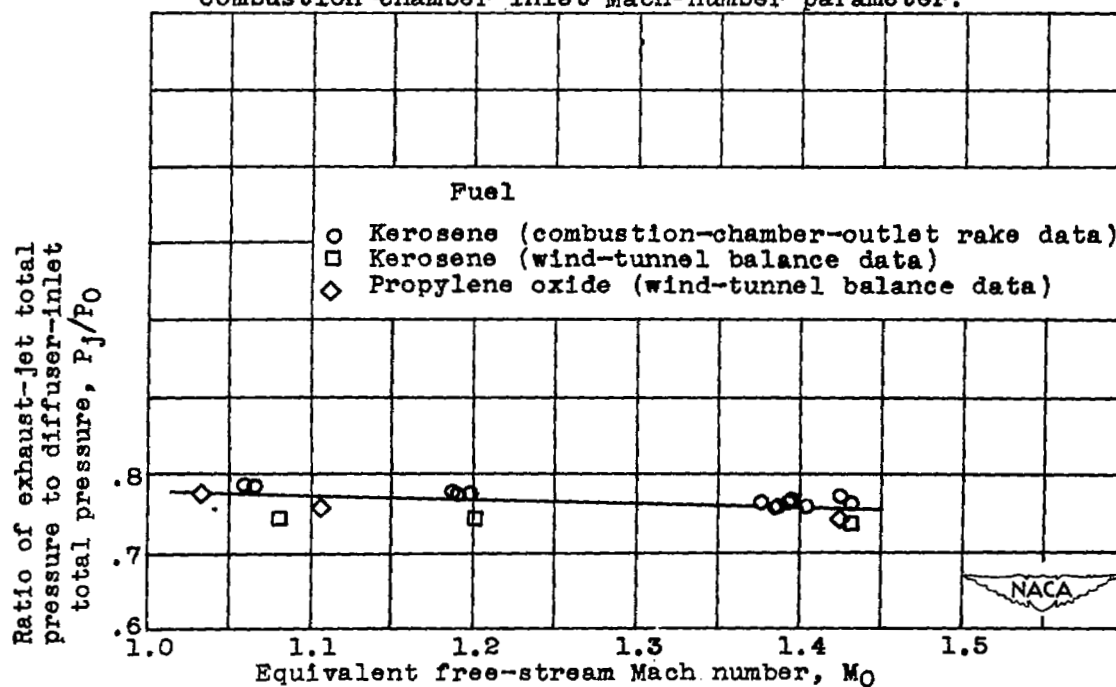
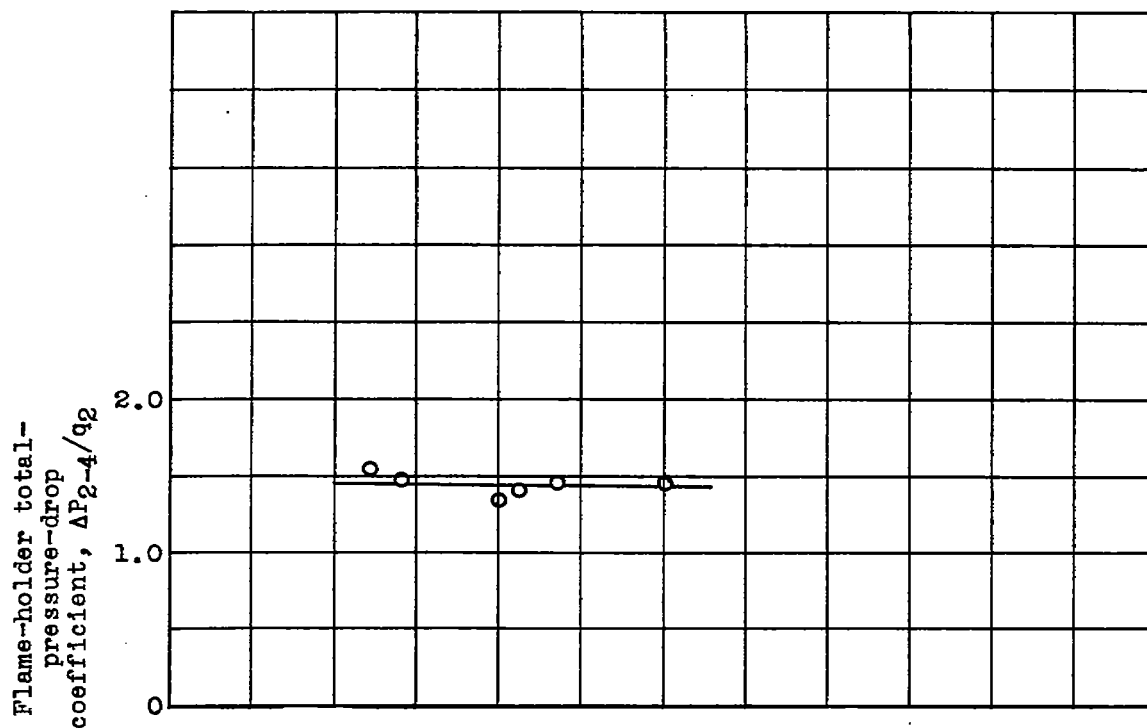
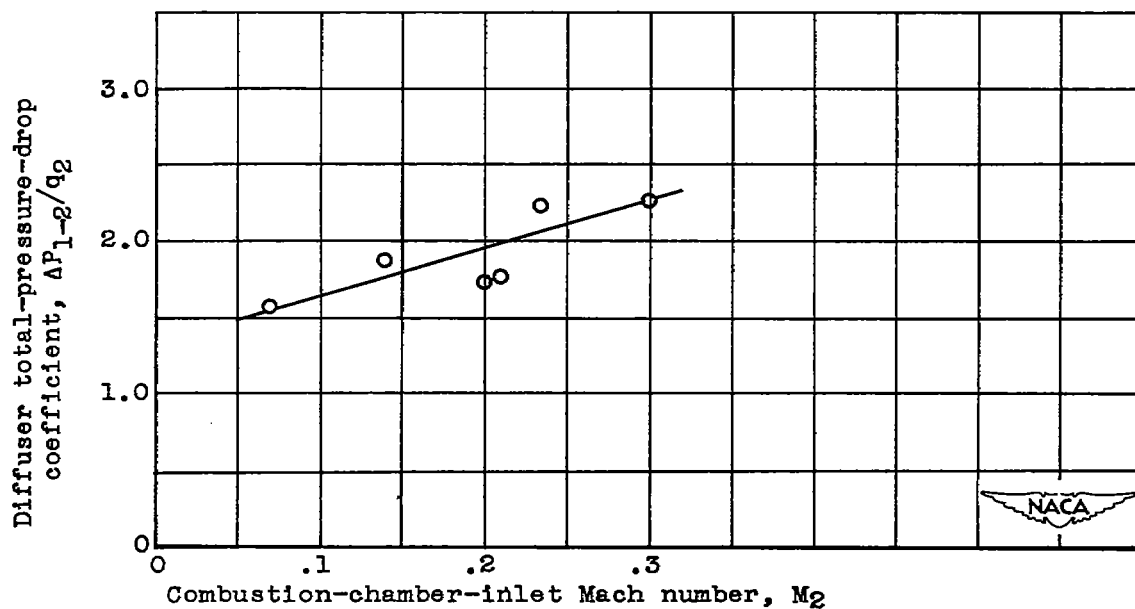


Figure 16. - Effect of equivalent free-stream Mach number on ratio of exhaust-jet total pressure to diffuser-inlet total pressure.



(a) Flame-holder total-pressure-drop coefficient.



(b) Diffuser total-pressure-drop coefficient.

Figure 17. - Effect of combustion-chamber-inlet Mach number on flame-holder and diffuser total-pressure-drop coefficients without combustion.



NASA Technical Library



3 1176 01435 5425

